

DMD # 84269

TITLE PAGE

Pharmacogenomic Next-Generation DNA Sequencing: Lessons from the Identification and Functional Characterization of Variants of Unknown Significance in *CYP2C9* and *CYP2C19*

Authors:

Dr. Sandhya Devarajan, Irene Moon, Dr. Ming-Fen Ho, Dr. Nicholas B. Larson, Drew R. Neavin,
Dr. Ann M. Moyer, Dr. John L. Black, Dr. Suzette J. Bielinski, Dr. Steven E. Scherer, Dr. Liewei
Wang, Dr. Richard M. Weinshilboum and Dr. Joel M. Reid

Department of Molecular Pharmacology and Experimental Therapeutics, Mayo Clinic,
Rochester, MN, USA (S.D, I.M, M.F.H, L.W, R.M.W, J.M.R)

Department of Health Sciences Research, Mayo Clinic, Rochester, MN, USA (S.J.B, N.B.L)

Personalized Genomics Laboratory, Department of Laboratory Medicine and Pathology, Mayo
Clinic, Rochester, MN, USA (J.L.B, A.M.M)

Department of Molecular Pharmacology and Experimental Therapeutics, Mayo Clinic Graduate
School of Biomedical Sciences, Mayo Clinic, Rochester, MN, USA (D.R.N)

Human Genome Sequencing Center, Department of Molecular and Human Genetics, Baylor
College of Medicine, Houston, TX, USA (S.E.S)

DMD # 84269

Running title: Functional characterization of *CYP2C9* and *CYP2C19* VUSs

Corresponding Author:

Dr. Joel M. Reid

Guggenheim 17-42C

Mayo Clinic, 200 First Street SW, Rochester, MN- 55905

Email: reid@mayo.edu

Phone: 507-284-4303

Word count:

Number of text pages: 38

Number of tables: 4

Number of figures: 5

Number of references: 55

Number of words in abstract: 249

Number of words in introduction: 732

Number of words in discussion: 1462

DMD # 84269

Abbreviations: BOMF, (benzyloxymethoxy) fluorescein; CDS, Clinical Decision Support; CL_{int}, Intrinsic clearance; CPR, cytochrome P450 oxidoreductase; CYP, Cytochrome P450; EHR, Electronic Health Record; eMERGE, Electronic Medical Records and Genomics network; EOMCC, 7-(ethoxymethoxy)-3-cyanocoumarin; FDA, Food Drug Administration; K_m, Michaelis constant; LC-MS/MS, Liquid Chromatography - Mass Spectrometry and Liquid Chromatography - Tandem Mass Spectrometry; MRM, Multiple Reaction Monitor; NHGRI, National Human Genome Research Institute; NGS, Next Generation Sequencing; ORF, Open Reading Frame; PGRN, Pharmacogenomics Research Network; PGx, Pharmacogenomics; SNPs, Single Nucleotide Polymorphisms; SRS, substrate Recognition Sites; The RIGHT Protocol, The Right Drug, Right Dose, Right Time- Using Genomic data to Individualize Treatment Protocol; V_{max}, velocity maximum; VUS, Variant of Unknown Significance; WT, Wild Type

DMD # 84269

Abstract

CYP2C9 and *CYP2C19* are highly polymorphic pharmacogenes, but clinically actionable genetic variability in drug metabolism due to these genes has been limited to a few common alleles. The identification and functional characterization of less common open reading frame sequence variation might help to individualize therapy with drugs that are substrates for the enzymes encoded by these genes. The present study identified seven uncharacterized variants each in *CYP2C9* and *CYP2C19* using next generation sequence data for 1013 subjects, and functionally characterized the encoded proteins. Constructs were created and were transiently expressed in COS-1 cells for the assay of protein concentration and enzyme activities using fluorometric substrates and LC-MS/MS with tolbutamide (*CYP2C9*) and (S)-mephenytoin (*CYP2C19*) as prototypic substrates. Results were compared with SIFT, Polyphen, and Provean functional prediction software. Cytochrome P450 oxidoreductase CPR activities were also determined. Positive correlations were observed between protein content and fluorometric enzyme activity for variants for *CYP2C9* (P<0.05) and *CYP2C19* (P<0.0005). However, *CYP2C9* 709G>C and *CYP2C19* 65A>G activities were much lower than predicted based on protein content. Substrate intrinsic clearance values for *CYP2C9* 218C>T, 343A>C and *CYP2C19* 337G>A, 518C>T, 556C>T and 557G>A were less than 25% of wild type (WT) allozymes. CPR activity levels were similar for all variants. In summary, sequencing of *CYP2C9* and *CYP2C19* in 1013 subjects identified low frequency variants that had not previously been functionally characterized. *In silico* predictions were not always consistent with functional assay results. These observations emphasize the need for high-throughput methods for pharmacogene variant mutagenesis and functional characterization.

DMD # 84269

Introduction

Pharmacogenomics (PGx) is the study of the role of genetic variation in variability in drug response phenotypes (Weinshilboum, 2003). Individual response to drug therapy varies widely, with genetic factors possibly accounting for 20% to 30% of that variation (Ingelman-Sundberg and Rodriguez-Antona, 2005). While genetic variants contribute to variability in function for genes encoding drug metabolizing enzymes, drug transporters, drug receptors, and signaling molecules, genes encoding drug metabolizing enzymes have received the most attention for clinical implementation, (Ingelman-Sundberg and Rodriguez-Antona, 2005; Weinshilboum and Wang, 2017). Significant associations of non-synonymous single-nucleotide polymorphisms (SNPs) in these genes with drug treatment outcomes are reported regularly (Sim et al., 2013). Genetic heterogeneity in genes encoding drug-metabolizing enzymes contributes to population heterogeneity in drug response by influencing both pharmacokinetics and pharmacodynamics (Dresser et al., 2000; Kim et al., 2008).

Cytochrome P450 enzymes in families 1-3 metabolize 70-80% of all clinically used drugs that undergo phase I metabolism (Ingelman-Sundberg et al., 2007; Sim et al., 2013). Nearly 40-45% of those drugs are cleared by oxidative metabolism catalyzed by CYP2C9, CYP2C19, and CYP2D6 (Kirchheiner et al., 2004). The genes encoding these CYPs have numerous polymorphisms, and those polymorphisms may have significant impact on the clinical effects of drugs with narrow therapeutic indices. Therefore, the US Food Drug Administration has adopted black box warnings for several narrow therapeutic index drugs, recommending PGx testing before prescribing these drugs. Similarly, many drugs with potentially promising efficacy never

DMD # 84269

reach the market because of adverse drug reactions or large variation in efficacy. It is possible that PGx variants may explain the large variation in response to drug treatment and predict adverse drug reactions (Friedman et al., 1999; Murphy, 2000).

Advanced sequencing technologies continue to identify variants in the drug-metabolizing enzyme genes that encode allozymes with poorly characterized or unknown clinical significance. Next Generation Sequencing (NGS) studies of large populations such as the 100,000 Genomes Projects (Mark et al., 2017) has generated DNA sequence data for PGx genes. Several years ago, the Mayo Clinic instituted the Right Drug, Right Dose, Right Time-Using Genomic Data to Individualize Treatment Study (RIGHT Protocol) in collaboration with the National Human Genome Research Institute (NHGRI), the Electronic Medical Records and Genomics (eMERGE) network, and the Pharmacogenomics Research Network (PGRN) (Bielinski et al., 2014). That project was designed to investigate the clinical implementation of preemptive PGx testing and provide clinicians with point of care PGx-guided prescribing information. Specifically, 1013 subjects gave permission for the sequencing of their DNA for 84 pharmacogenes among which *CYP2C19*, *CYP2C9*, *VKORC1*, *CYP2D6*, and *SLCO1B1* are incorporated into the electronic health record (EHR) (Ji et al., 2016).

The RIGHT study identified a series of rare variants in the open reading frames (ORFs) of *CYP2C9* and *CYP2C19*. Those variants either lacked functional characterization or had not been previously reported. The standard strategy to identify the functional significance of variants begins with the preparation of recombinant allozymes using site directed mutagenesis followed

DMD # 84269

by expression in human cell lines, measurement of protein concentrations, and determination of enzyme activity using prototypic substrates (Dai et al., 2014a; Dai et al., 2015; Dai et al., 2014b; DeLozier et al., 2005; Hu et al., 2015; Niinuma et al., 2014; Wang et al., 2005; Wang et al., 2003; Weinshilboum et al., 1999). Computational methods have also been developed in an attempt to predict the effect of genetic variation in encoded amino acid sequence on protein stability and enzyme activity, but their validation and accuracy remains unclear (Flanagan et al., 2010).

The present study was designed to determine the functional effect of rare variants found in both *CYP2C9* and *CYP2C19* in the RIGHT sequence data. We utilized a standard approach to prepare recombinant variant allozymes and studied the effect of those variants on protein level and enzyme activity using both fluorescent probe substrates and prototypic substrates. The functional consequences of many of the variants could not be accurately predicted by current algorithms. Study of these variants showed functional effects that might indicate clinical utility with regard to variation in drug response phenotypes. If these results can be generalized, they indicate that, ultimately, DNA sequencing will be preferable to genotyping for the clinical implementation of pharmacogenomic variants, and they also strongly support the need for high throughput functional assays and accurate predictive algorithms in order to make it possible to achieve the optimal reduction in adverse drug reactions and the optimal increase in drug efficacy that pharmacogenomics promises.

DMD # 84269

Materials and methods

Study subjects

The Right Study enrolled 1013 participants and sequenced 84 pharmacogenes for each subject. This study was conducted according to the Declaration of Helsinki and was reviewed and approved by the Mayo Clinic Institutional Review Board. The subjects were 86% non-Hispanic white and 53% were women with 96.7% white, 1% Asian, 0.6% African American, 0.1% American Indian/Alaskan Native, 0.5% other race and 1.1% unknown or chose not to disclose their ethnicity (Bielinski et al., 2014; Ji et al., 2016).

***CYP2C9* and *CYP2C19* gene sequencing**

PGx gene capture and NGS of DNA was conducted in the Personalized Genomics Laboratory and Clinical Genome Sequencing Laboratory, Mayo Clinic, Rochester, MN. The PGRN-Seq capture reagent V1.0 was used to sequence 84 pharmacogenes and covered 968 kilobases (kb) that included approximately 2kb upstream and downstream of the coding regions of these genes (Ji et al., 2016). The KAPA HTP Library Preparation Kit (Kapa Biosystems, Inc., Wilmington, MA) and Bioo Scientific NEXTflex barcode adapters (Bioo Scientific Corporation, Austin, TX) were used for library preparation and precapture pooling. Samples were sequenced using the Illumina HiSeq2500 Sequencing System in the rapid run mode by using the TruSeq Rapid SBS Kit (Illumina, San Diego, CA) with the 200-cycle and 2 X 101 pair end reads capability (Ji et al., 2016). FASTQC was used to assess raw read quality. Files were aligned to the hg19 reference

DMD # 84269

genome using Novoalign (VN:V2.07.13). Single-nucleotide variants were identified by CLC's Neighborhood Quality calling method.

Specific regions around known *CYP2C9* and *CYP2C19* alleles were examined, and Sanger sequencing was used to confirm observed variants. Each variant was confirmed 10 times. The NGS workbench, which is an internally-developed Mayo Clinic program that facilitates results interpretation, was used to review quality metrics and to manually annotate novel or ambiguous sequence alterations (Bielinski et al., 2014).

***CYP2C9* and *CYP2C19* cDNA expression constructs**

Human *CYP2C9* cDNA and human *CYP2C19* cDNA clones in the eukaryotic expression vector pCMV6-XL5 were obtained from OriGene Technologies, Inc (Rockville, MD). Site-directed mutagenesis was then performed using the QuikChange Lightning kit (Agilent Technologies, Santa Clara, CA) to create expression constructs for each of the variants to be studied. Sequences of the primers used to perform site-directed mutagenesis are listed in the Supplemental material (**Supplemental Tables 1 and 2**). The sequences of the human *CYP2C9* cDNA and *CYP2C19* cDNA clones and all variant constructs were also confirmed by Sanger sequencing.

Expression of *CYP2C9* and *CYP2C19* variant proteins in COS-1 cells

COS-1 African green monkey kidney cells do not express *CYP2C9* or *CYP2C19* and, as a result, were selected for use in our expression studies. Specifically, the cells were grown in Dulbecco's modified Eagle's medium (DMEM) supplemented with 10% fetal bovine serum. At 24 hours before transfection, the cells were plated at a density of 1.25×10^6 per T75 flask. Subsequently,

DMD # 84269

the cells were transfected with plasmids carrying *CYP2C9* or *CYP2C19* cDNA using Lipofectamine 3000 (Invitrogen, Carlsbad, CA) according to the manufacturer's instructions. After 6 hours of incubation at 37°C, the culture medium was replaced with DMEM containing 10% fetal bovine serum, and the cells were incubated for an additional 66 hours. Each expression clone was homozygous for the nucleotide change. The cells were then washed with PBS, followed by trypsinization and pelleting in PBS (2000 rpm centrifugation for 10 min at 4°C) for S9 fractionation.

Preparation of S9 fractions of cell pellets

Cells were resuspended in 300 µl of 0.25M sucrose. After sonication for 20 seconds using a probe sonicator and centrifugation at 2500 rpm for 5 minutes, the supernatant was transferred to a new tube and centrifuged at 9000 rpm for 10 minutes. The resulting supernatant was transferred to a microcentrifuge tube. The DC protein Assay kit (catalog number 800- 0112; Bio Rad, Hercules, CA, USA) was used to measure the protein content of the S9 fractions.

Western blot analysis

Quantitative Western blot analyses were performed using *CYP2C9* or *CYP2C19* S9 fractions.

Proteins were separated by SDS-PAGE prior to transfer to PVDF membranes. The membranes were incubated with rabbit polyclonal *CYP2C9* antibody (Abcam, Cat. No. ab4236) or *CYP2C19* antibody (Sigma, Cat. No. SAB2100520) at a 1:1,000 or 1:250 dilution, respectively. ACTB protein was measured using mouse monoclonal ACTB antibody (Sigma, Cat. No.

DMD # 84269

A1978), and its expression was used as a loading control. The expression of each variant was normalized with regard to that of the wild-type. Proteins were detected using the SuperSignal™ West Dura Extended Duration Substrate (Thermo Scientific, Rockford, IL), and images were captured on X-ray films. Quantification of protein density on X-ray films was performed with NIH ImageJ software (<https://imagej.nih.gov/ij/download.html>).

Protein degradation experiments

In some experiments, cells were treated with 10 μ M 3-methyladenine (3MA; Selleckchem, Houston, TX) for 48 hours, or 10 μ M carbobenzoxy-L-leucyl-L-leucyl-L-leucinal (MG132; a proteasome inhibitor; Selleckchem, Houston, TX) for 8 hours to determine whether CYP2C9 and CYP2C19 variant allozymes might be degraded by either autophagy (3MA) or by a proteasome-mediated process (MG132) in COS-1 cells (Ji et al., 2007; Liu et al., 2017; Pereira et al., 2010; Wang et al., 2005; Wang et al., 2004). The cells were then collected for S9 fractionation.

Enzyme assays

CYP2C9 and CYP2C19 enzyme activities were measured using a modification of the Vivid® assay (Vivid®, Cat. No. P2860 and P2864). In this assay, blocked dye substrates, BOMF and EOMCC for the CYP2C9 and CYP2C19 enzymes respectively, were metabolized into fluorescent products in an aqueous solution. In our experiments, we incubated CYP2C9 and CYP2C19 S9 fractions at protein concentrations of 4.8mg/100ul and 3.9mg/100ul, respectively, with an NADPH regeneration system consisting of glucose 6-phosphate and glucose- 6-

DMD # 84269

phosphate dehydrogenase and reaction buffer which were included in the kit, at room temperature in triplicate for 20 minutes in 96 well plate. The enzyme reaction was initiated by the addition of a mix of NADP⁺ and appropriate vivid substrates concentration (2uM of Vivid[®] BOMF substrate, Cat. No. P2869 for CYP2C9 and 10uM of Vivid[®] EOMCC substrate, Cat. No. P3024 for CYP2C19- which are provided in the kit). Immediately (less than 2 minutes) after initiation of the enzyme reaction, fluorescent products were measured at intervals of 15 minutes spectrophotometrically at excitation /emission wavelengths of 490/520nm for CYP2C9, and 415/460nm for CYP2C19 substrates, against Vivid[®] fluorescent standard concentrations of 500 nM, 250 nM, 125 nM, 62.5 nM, 15.625 nM, 7.8125 nM and 0 nM in duplicate wells. Relative enzyme activities were measured compared to WT activity as 100%. Enzyme activity of all variant allozymes of CYP2C9 and all variant allozymes of CYP2C19 were conducted on the same day at the same time alongside their respective WT enzymes.

CYP2C9 and CYP2C19 enzyme kinetic parameters were characterized with tolbutamide and (S)-mephenytoin, respectively, as substrates. Specifically, S9 fractions of CYP2C9 and CYP2C19 enzyme suspensions were incubated in a 2 ml micro centrifuge tube maintained at 37°C in a shaker bath. Each incubation mixture (100 µL) contained S9 fraction (0.4 mg/ml protein final concentration), NADPH (1 mM), magnesium chloride (5 mM) and potassium phosphate buffer (50 mM pH 7.5, CYP2C9) or Tris buffer (100 mM pH 7.4, CYP2C19). Identical S9 incubations in which NADPH was omitted served as controls. After pre-incubation of the S9 with the reaction buffer (+/- NADPH) for two minutes, the metabolic process was initiated by adding tolbutamide (CYP2C9) or (S)-mephenytoin (CYP2C19) for a final concentration of 1000, 500, 100, 50 and 10 µM. Reactions were terminated after 30 minute incubations by mixing with ice-cold methanol (2:1, v/v) containing 282 nM (hydroxy tolbutamide-d9) or 354 nM ((+/-)-4-

DMD # 84269

hydroxy mephenytoin-d3) internal standards and were vortexed for 1 minute before centrifugation at 14,000 g for 15 minutes. The resultant supernatant was collected for LC/MS/MS analysis.

Cytochrome P450 oxidoreductase activity was measured in the S9 fraction of cells in which *CYP2C9* and *CYP2C19* variant allozymes had been expressed using a colorimetric Cytochrome P450 reductase Activity Assay Kit (abcam, Cat. No. ab204704). This assay uses the oxidation of NADPH catalyzed by cytochrome P450 reductase to cause the conversion of a nearly colorless probe substrate into a brightly colored product with an absorbance at OD_{460nm} wavelength. A G6P standard curve preparation of 0, 2, 4, 6, 8 and 10 nmol/well in a 96 well plate was used. In order to subtract any extraneous reductase activity in samples, all variant samples were assayed in parallel with the presence and absence of 0.1mM Diphenyleneiodonium Chloride, an inhibitor of NADPH- dependent flavoprotein, subtracting any residual activity detected with the inhibitor present. The optical density was measured using a spectrophotometer in kinetic mode for 30 minutes. The CPR activity was calculated between two time points in the linear range. The rate of color formation is directly proportional to cytochrome P450 oxidoreductase activity. Activity was expressed as mU per mg of total protein. One Unit CPR activity equals to the amount of Cytochrome P450 Reductase that will generate 1.0 μ mol of reduced substrate per minute by oxidizing 1.0 μ mole NADPH to β -NADP⁺ at pH 7.7 at 25°C.

Drug analysis using LC-MS/MS assay

Tolbutamide, hydroxy tolbutamide, hydroxy tolbutamide-d9, (S)-mephenytoin, (S)-4-hydroxy mephenytoin, and (+/-)-4-hydroxy mephenytoin-d3 (used for IS) were obtained from Toronto

DMD # 84269

Research Chemicals (Toronto, ON, Canada). HPLC-grade methanol and water were purchased from EM Science (Gibbstown, NJ, USA). Formic acid (minimum 95%), dimethyl sulfoxide (DMSO), β -nicotinamide adenine dinucleotide phosphate reduced form (NADPH), potassium phosphate dibasic, potassium phosphate monobasic, and magnesium chloride were purchased from Sigma (St. Louis, MO, USA). Phosphate buffered saline was purchased from Invitrogen (Carlsbad, CA, USA). Tris HCL buffer 10X solution was purchased from Sigma. Sodium hydroxide solution was purchased from Sigma Aldrich. Deionized and distilled water was used to prepare buffer solution.

Stock solutions of 1mg/ml of tolbutamide, hydroxy tolbutamide, hydroxyl tolbutamide-d9, (S)-mephenytoin, (S)-4-hydroxy mephenytoin, (+/-)-4-hydroxy mephenytoin-d3 were prepared in methanol and were stored at -20°C . 20X stock solutions of concentration 2.9 nM, 14.6 nM, 29.1 nM, 58.2 nM, 146 nM, 291 nM, 1455 nM, 2910 nM for hydroxy tolbutamide and 3.6 nM, 17.8 nM, 35.6 nM, 71.1 nM, 178 nM, 356 nM, 1789 nM, 3558 nM for (S)-4-hydroxy mephenytoin were prepared by diluting the 1mg/ml stock solutions with 1: 1 methanol: water and were stored in -20°C . Standard samples and QC's (hydroxy tolbutamide- 8.7 nM, 218 nM, 2182 nM and (S)-4-hydroxy mephenytoin - 10.7 nM, 267 nM and 2668 nM concentration) were prepared in assay buffer containing 0.4mg of protein (bovine serum albumin). Incubations of triplicate standard curves, QC's and samples mixtures were performed at 37°C in a total volume of 100ul. Interday and Intraday variability for CYP2C9 and CYP2C19 standard curves were $<25\%$ for their respective lowest standard. The concentration range of samples for CYP2C9 and CYP2C19 were 0- 178 nM and 0- 694 nM, respectively.

DMD # 84269

The separation of tolbutamide, hydroxy tolbutamide, hydroxy tolbutamide-d₉, (S)-mephénytoin, (S)-4-hydroxy mephénytoin, and (+/-)-4-hydroxy mephénytoin-d₃ was achieved with a precolumn filter (Column Saver, MAC-MOD Analytical, Inc, Chadds Ford, PA) and a Waters select HSS T3 column (2.1 × 100 mm, XP, 2.5µm) (Waters Corporation, Milford, MA, USA) by gradient elution utilizing the following profile: 2-6 minute 75% A and 25% B, 6-8 minutes 5% A and 95% B, 8-10 minutes 75% A and 25% B, where solvent A was water containing 0.1% formic acid and solvent B was methanol containing 0.1% formic acid. The flow rate was 0.2 ml/min. After sample injection (20 µL), the column effluent was diverted to waste for 3 minutes, after which the flow was switched to the mass spectrometer.

Metabolites of tolbutamide and (S)-mephénytoin were monitored using a modification of a previously published LC-MS/MS assay (Peng et al., 2015). The LC/MS/MS system used to perform the assays consisted of a Shimadzu liquid chromatograph (Wood Dale, IL, USA) with two LC-10ADvp pumps (flow rate 0.200 mL/min), and an SIL-10ADvp auto-injector (injection volume 20 µL) coupled to a Quattro Micro mass spectrometer fitted with an electrospray ionization (ESI) probe (Waters Corporation, Milford, MA). Hydroxy tolbutamide detection was accomplished using multiple reaction monitoring (MRM) in positive ESI mode with parent ion of 287.1 m/z, daughter ion 74.1m/z, dwell 0.1sec, cone 28 volts, and collision energy 13eV. Internal standard (hydroxy tolbutamide-d₉) detection was performed using MRM in positive ESI mode with parent ion of 296.1 m/z, daughter ion of 83.2 m/z, dwell 0.1 sec, cone 30 volts, and collision energy 14 eV. (S)-4-hydroxy mephénytoin detection was accomplished with parent ion of 235.1 m/z, daughter ion of 150.2 m/z, dwell 0.1 sec, cone 19eV. Internal standard ((+/-)-4-hydroxy mephénytoin-d₃) detection was performed using MRM in positive ESI mode with parent ion of 238.2 m/z, daughter ion of 150.2 m/z, dwell 0.1 sec, cone 19eV. The source

DMD # 84269

temperature, desolvation temperature, cone gas flow, and desolvation gas flow were 120°C, 350°C, 650L/hr and 25L/hr, respectively. MS data were collected for 10 minutes after injection. Spectra and chromatograms were processed using the MassLynx v3.5 software (Waters Corporation, Milford, MA). Metabolism data were acquired using a full scan function (MS scan) over the range of potential metabolites (50 - 450 m/z). Once the metabolite masses were determined, a daughter ion scan was performed to determine and confirm the structure of the metabolite.

***In silico* variant sequence prediction analysis**

Polymorphism Phenotyping v2 (Polyphen 2) (Adzhubei et al., 2010), Protein Variation Effect Analyzer (PROVEAN) (Choi and Chan, 2015) and Sorting Intolerant From Tolerant (SIFT) (Sim et al., 2012) – three commonly-used, publically-available variant effect prediction tools—were utilized in order to predict the functional impact of the novel variants identified across *CYP2C9* and *CYP2C19*. The web server versions of these tools were used under their default settings.

Statistics

Protein expression data were analyzed using GraphPad Prism7 software (GraphPad Software, La Jolla, CA). Data were displayed as mean \pm S.E.M. Protein expression was analyzed using ANOVA followed by appropriate post hoc tests for multiple comparisons. A value of $p < 0.05$ was considered statistically significant. Enzyme activity was analyzed using one-way ANOVA, with mean comparison for each variant genotype against the wildtype control performed using

DMD # 84269

Dunnet's test. Corresponding p-values were multiplicity-adjusted and reported as such. Associations between protein content and enzyme activity were evaluated using Pearson correlations, with two-sided t-test p-values reported. Enzyme kinetics were modeled using non-linear regression based on the Michaelis-Menten equation. All p-values less than 0.05 were considered statistically significant. Analyses were performed using GraphPad Prism version 7.

Results

Variants in *CYP2C9* and *CYP2C19*

Sequencing of the DNA from the 1013 subjects enrolled in the RIGHT Study identified seven heterozygous variants in the *CYP2C9* gene and seven variants in the *CYP2C19* gene (**Table 1**) that are not included in current clinical algorithms or guidelines for the metabolic phenotypes of these enzymes. The gnomAD and dbSNP databases were searched for previous reports of these variants and the results are listed in **Table 2**. For *CYP2C9*, variant 218C>T was found in our cohort with a heterozygous *CYP2C9**2 allele. *CYP2C9* variants 229C>A and 709G>C are variants that had not been reported in the gnomAD or dbSNP databases. For *CYP2C19*, variant 65A>G was found together with heterozygous *CYP2C19**17; variant 337G>A was found with heterozygous *CYP2C19**2 and *CYP2C19**17; variants 518C>T and 578A>G were found with heterozygous *CYP2C19**2; and variants 556C>T and 557G>A were found with homozygous *CYP2C19**2. Variant 815A>G is a variant that had not been reported in the gnomAD or dbSNP databanks.

DMD # 84269

Changes in gene expression by novel *CYP2C9* and *CYP2C19* variants

As a first step in our functional analysis, we sought to determine if the variants found in both *CYP2C9* and *CYP2C19* would influence protein expression and the enzyme activity of allozymes encoded by the variant sequences. Each expression clone was homozygous for the nucleotide change. Quantitative western blot analysis of protein expression showed reduced expression of *CYP2C9* protein for three of the identified *CYP2C9* variants (229C>A, 709G>C and 801C>T) (**Figure 1A**). In a similar fashion, quantitative western blot analysis of Protein expression showed reduced expression of *CYP2C19* protein for four of the identified *CYP2C19* variants (65A>G, 337 G>A, 578A>G and 815A>G), as well as in loss of function variants *CYP2C9**3 (Andersson et al., 2012; Lee et al., 2014; Prieto-Perez et al., 2013) and *CYP2C19**3 (Scott et al., 2011; Scott et al., 2013) (**Figure 1A**).

We next set out to determine mechanism(s) responsible for the decreased protein levels of *CYP2C9* or *CYP2C19* variant allozymes. Accelerated protein degradation is a common mechanism that can contribute to decreased levels of protein, either as a result of ubiquitin-proteasome or autophagy-mediated degradation (Deng et al., 2016; Li et al., 2008). Therefore, we tested the effect of an autophagy inhibitor (3MA) and a proteasome inhibitor (MG132) on protein expression levels of selected variants allozymes with levels that were decreased to at least 50% or less as compared to the WT allozymes (**Figure 1B**). Strikingly, three variants for *CYP2C9* and two variants for *CYP2C19* displayed significantly increased protein expression, as compared to baseline, after treatment with MG132. Although it was not statistically significant,

DMD # 84269

we also noticed that both CYP2C9 and CYP2C19 WT protein levels increased in response to exposure to MG132—suggesting that the proteasome may play a role in basal levels of protein expression for these enzymes. These observations suggest that several of the variants for both enzymes undergo accelerated proteasome-mediated degradation. Finally, protein levels for none of the variant allozymes were significantly affected by treatment with 3MA (**data not shown**).

Changes in enzyme activity in novel CYP2C9 and CYP2C19 variants

Enzyme activity levels for these same preparations were determined using the fluorogenic Vivid[®] substrates, and those results are shown in **Figure 2A** and **2B**, respectively. These results were generally comparable with results of the protein expression studies (**Figure 1A**) with some notable exceptions. For example, CYP2C9 709G>C and CYP2C19 65A>G displayed significantly reduced enzyme activity, but their protein level was similar to that of the WT allozyme. The reduced activity could be due to changes in the nucleotide sequence near active site affecting the enzyme activity more than protein level. Overall, there was a significant positive correlation between levels of enzyme activity and protein content for both CYP2C9 ($p=0.0015$; $r^2=0.693$) and CYP2C19 ($p=0.0003$; $r^2=0.825$), as shown graphically in **Figures 3A** and **3B**, respectively.

The enzyme activities of CYP2C9 and CYP2C19 variant allozymes expressed in COS-1 cells were also determined with the prototypic substrates tolbutamide and (S)-mephenytoin, respectively. The concentration range of product formation in samples for CYP2C9 and CYP2C19 were 0- 178 nM and 0- 694 nM, respectively. Michaelis-Menten plots for tolbutamide (CYP2C9) and (S)-mephenytoin (CYP2C19) are shown in **Figures 4A** and **4B**, respectively.

DMD # 84269

Kinetic parameters for recombinant CYP2C9 variant allozymes as well as empty vector (EV), WT, and CYP2C9*3 as negative controls, are listed in **Table 3**. Similarly, kinetic parameters for recombinant CYP2C19 variants together with EV, WT, and CYP2C9*3 as negative control are shown in **Table 4**. For *CYP2C9*, we found that the catalytic activities of variants were less than 25% for 218C>T, 343A>C, 707delA, 707_709delinsCC, 25-50% (intermediate activity) for variants 709G>C, 791T>C and 50-100% (equal or similar to WT) for 229C>A and 801C>T when compared to that of the WT allozyme. Similarly the catalytic activities of CYP2C19 variants were less than 25% for 337G>A, 518C>T, 556C>T and 557G>A; 25-50% (intermediate activity) for variants 65A>G and 815A>G and 50-100% (equal or similar) for 578A>G when compared to that of the WT allozyme. There was a significant positive correlation between enzyme activities determined using the Vivid[®] reagent and velocity of product formation at 50 μ M drug concentration for CYP2C9 ($p = <0.0001$; $r^2=0.907$) and 1000 μ M drug concentration for CYP2C19 ($p = <0.0001$; $r^2=0.898$), as shown in **Figures 5A** and **5B**, respectively.

Cytochrome P450 oxidoreductase (CPR) activities in majority of the cells transfected with CYP2C9 variant allozymes were similar to those for the CYP2C9 WT allozymes, as expected. In a similar fashion, cells transfected with CYP2C19 variant allozymes showed CPR activities similar to those observed in cells transfected with the CYP2C19 WT allozymes, as shown graphically in supplemental material (**Supplemental Figures 1A** and **1B** respectively).

***In silico* variant sequence prediction analysis**

The impact of *CYP2C9* and *CYP2C19* variant sequence on enzyme activity was predicted *in silico* using Polyphen, SIFT and Provean (Adzhubei et al., 2010; Choi and Chan, 2015; Sim et

DMD # 84269

al., 2012) (**Table 4 and Table 5, respectively**). The three programs predicted no effects (benign/ tolerated/ neutral) for 1/7 *CYP2C9* and 2/7 *CYP2C19* variants and loss of function (probably damaging, damaging, deleterious) for 2/7 *CYP2C9* and 1/7 *CYP2C19* variants. Concordance, defined as agreement of the kinetic assay result with at least two of three *in silico* software results, was observed for nine of fourteen variants. Predictions differed among the programs for *CYP2C9* variants 229C>A, 791T>C and *CYP2C19* variants 65A>G, 518C>T, 557G>A and 815A>G. Furthermore, there were difference between programs and functional assay results, for example, *CYP2C9* variant 709G>C, which had low catalytic activity (< 50% of WT), was predicted by Polyphen, SIFT and Provean (Adzhubei et al., 2010; Choi and Chan, 2015; Sim et al., 2012) to be “benign”, “tolerated” and “neutral”, respectively. Similarly, *CYP2C19* variant 65A>G, which had low catalytic activity (< 50% of WT), was predicted by Polyphen, SIFT and Provean (Adzhubei et al., 2010; Choi and Chan, 2015; Sim et al., 2012) to be “benign”, “tolerated” and “deleterious”, respectively.

Discussion

PGx will be the first aspect of clinical genomics to achieve broad clinical implementation, eventually touching virtually all patients (Weinshilboum and Wang, 2017). In the Mayo Clinic RIGHT1K study, NGS was performed for 1013 participants to identify sequence variation in 84 pharmacogenes (Bielinski et al., 2014). We identified six non-synonymous ORF variants in the *CYP2C9* gene and seven in the *CYP2C19* gene. Expression of these variants after transfection into COS-1 cells most often yielded differing protein levels for variants allozymes as compared to the WT sequence. Using fluorometric probe and prototypical substrates to assess the impact of

DMD # 84269

these genetic polymorphisms on biological function, we observed substantial variability in enzyme activity among the variants that generally correlated with protein expression levels. We also observed a significant correlation between protein expression levels and Vivid[®] enzyme activities for CYP2C9 and CYP2C19. These results suggest that decreased protein level may be the major factor responsible for the decreased enzyme activity which we observed. That conclusion is consistent with protein degradation as a result of misfolding due to alteration in the amino acid sequence that leads to decreased protein levels for the variant enzyme—as has been observed in the past for variant allozymes as a result of non-synonymous SNPs (Li et al., 2008; Wang et al., 2005; Wang et al., 2003).

We also studied the impact of these polymorphisms on enzyme kinetics using the clinically relevant prototypic drug substrates tolbutamide and (S)-mephenytoin for CYP2C9 and CYP2C19, respectively. Three of seven CYP2C9 variant allozymes had low catalytic activity (<25%), two of seven had intermediate activity (25-50%) and two of seven had similar activity (50-100%) to WT. Similarly, four of seven CYP2C19 variant allozymes had low catalytic activity (<25%), two of seven had intermediate activity (25-50%) and one of seven had similar activity (50-100%) to WT. In addition, we found a significant correlation between our Vivid[®] fluorometric high throughput assay and enzyme kinetics of the prototypical substrates.

The COS-1 cell expression system used in this study to test recombinant enzymes does not constitutively express CYP enzymes, but does sufficiently express CPR and cytochrome b₅

DMD # 84269

enzymes to support CYP activities (Gonzalez and Korzekwa, 1995). Oxidation and reduction reactions supported by P450s require interactions between the P450 with CPR flavoprotein and NADPH. Changes in the level of CPR could potentially affect drug disposition (Backes and Kelley, 2003). Because cytochrome b₅ is not necessary in systems that co-express CPR and CYP2C9 or CYP2C19 (Yamazaki et al., 2002) and the COS-1 expression system yields small amounts of protein, it was not measured in this study. Since CPR is important and difference in expression may alter CYP2C9 and CYP2C19 activity, we measured CPR enzyme activity in all of the CYP2C9 and CYP2C19 variant samples. The observation of similar CPR activity among the recombinant samples suggests that variation in CPR levels is likely a minor factor in affecting CYP enzyme activity. While we cannot rule out variation in the nature of the interaction between the cytochromes P450 that we studied and CPR due to sequence variation in the cytochrome P450s, our results strongly suggest that protein degradation is a major factor for this variation in intrinsic clearance.

In silico predictions have been widely applied to genetic variation in structure and function of proteins. When we compared our enzyme kinetic results with *in silico* predictions, we found several differences between our functional results and the *in silico* predictions. For example, the CYP2C9 variant 709G>C was predicted to be benign, whereas functional studies with a prototypic substrate showed only 27% of the WT enzyme activity. Polyphen 2, SIFT and Provean are only three of a large number of programs designed to predict the effects of non-synonymous ORF SNPs, but our results—and those of others (Flanagan et al., 2010; Min et al.,

DMD # 84269

2016)--support the importance of functional studies as the “gold standard” for the functional assessment of variants that alter encoded amino acid sequence.

Gotoh has proposed six putative substrate recognition sites (SRSs) in mammalian P450s (Gotoh 1992), including SRS-1 (B-C loop), 2 (F-helix), 3(G-helix), 4 (I-helix), 5 (β 3 area) and 6 (C-terminal β -strand region 4 β 5) (Gotoh, 1992). These SRSs constitute about 76-79 amino acids and afford the structural, and functional basis for drug and enzyme alignment (Gotoh, 1992). Furthermore, non-synonymous mutations appeared to be more frequent within SRSs. Polymorphisms within SRS regions could cause protein structure conformational changes (Wester et al., 2004) and disrupt hydrophobic interactions with drug substrates (Straub et al., 1994). Earlier studies indicate that even single mutations at key residues result in significant geometrical alterations to substrate binding regions (Negishi et al., 1996). Thus, variant nucleotides may cause conformational changes in the enzyme, alter substrate binding affinity at the active site, and cause differences in enzyme activity. In our experiments, *CYP2C9* variant 218C>T occurs in SRS region 1, variant 343A>C occurs in SRS 3 region and variants 707delA, 709G>C, 707_709delinsCC occur in SRS 2 and SRS 3. Each of these alterations in amino acid sequence results in a significant reduction (<25%) in enzyme activity when compared to the WT sequence. Similarly, *CYP2C19* variant 337G>A occurs in SRS 1 and showed only ~10% of the *CYP2C19* WT activity for (S)-mephenytoin hydroxylation, but ~80% activity in our fluorometric assay, which might be explained by the substrate specificity of these enzymes. Obviously, the role of genetic variants in altering the physiochemical and structural properties of substrate binding sites and substrate affinity in different P450-substrate interactions requires further study.

DMD # 84269

However, *in vivo* studies in animals and humans are difficult, since many of these variants are rare and testing them *in vivo* would be expensive and time consuming. Therefore, the incorporation of the results of functional studies such as those described here into pharmacogenomic variant analysis for clinical purposes is essential in order to predict patient phenotypes and to allow for the use of clinical decision support tools that are currently being built into electronic health records.

The standard method to determine the effect of genetic variation on enzyme function involves cDNA expression in COS/yeast /insect/human cells, followed by characterization of enzyme kinetics. This approach has both strengths and limitations. The strengths include the fact that enzyme kinetic studies using prototypic substrates are clinically relevant and the results are closer to biological enzyme activity than many other characterization studies. The limitations of this approach include the fact that these studies are laborious and time consuming, making their use in high throughput assays difficult. Given the overwhelming number of new variants being identified, the time-consuming nature of standard methods of functional characterization and the limited accuracy of computational *in-silico* predictions, other approaches such as CRISPR Cas9 techniques (Guo et al., 2018) which are used to create genetic variants and recombinants, as well as techniques such as massively parallel single nucleotide mutagenesis (Haller et al., 2016) are being tested for functional genomic applications. Similarly, high throughput screening methods should be developed to make it possible to rapidly screen variants for their functional effects (Cheng et al., 2009; D. et al., 2008; G. et al., 2010; Kariv et al., 2001; Stresser et al., 2000; V Trubetskoy et al., 2005).

DMD # 84269

In summary, we have identified 13 non-synonymous ORF variants and one ORF synonymous variant in two important, clinically actionable pharmacogenes, *CYP2C9* and *CYP2C19*.

Functional studies of these variants showed impaired metabolism by the encoded allozymes which may be due, at least in part, to effects on protein stability, resulting in decreased metabolism of the drug substrate. These results serve to emphasize the need for high throughput functional genomic methods to address the tidal wave of novel variants discovered as pharmacogenomics moves from genotyping common variants that have been previously identified and functionally tested to preemptive sequencing. The move to preemptive NGS in ever larger population cohorts will identify ever larger numbers of variants with functional effects. For example, the Mayo Clinic has expanded the initial RIGHT protocol to an additional 10,085 patients, while variants identified in the 100,000 Genomes Project and those already present in GnomAD represent only two of the larger population cohorts that have become available. The application of standard approaches to study the functional effects of pharmacogene variants discovered during these studies will not be practically possible.

Therefore, novel robust high throughput methods are needed to identify nucleotide alterations that affect enzyme function, prepare recombinant enzymes that incorporate those alterations, and rapidly characterize the functional effects on enzyme activity resulting from those alterations. If the present results can be generalized, they suggest that, ultimately, DNA sequencing will be preferable to genotyping for the clinical implementation of pharmacogenomic variants, and they also support the need for high throughput functional assays and highly accurate predictive algorithms if we are to achieve the optimal decrease in adverse drug reactions and the optimal increase in drug efficacy that PGx promises.

DMD # 84269

Acknowledgements

T32 GM072474

Authorship contributions

Participated in research design: Reid, Wang, Weinshilboum, Devarajan, and Moon

Conducted the experiments: Devarajan, and Moon

Performed data analysis: Devarajan, and Moon

Wrote or contributed to the writing of the manuscript: Devarajan, Moon, Ho, Larson, Black, Bielinski, Neavin, Moyer, Scherer, Wang, Weinshilboum and Reid

DMD # 84269

References:

- Adzhubei IA, Schmidt S, Peshkin L, Ramensky VE, Gerasimova A, Bork P, Kondrashov AS and Sunyaev SR (2010) A method and server for predicting damaging missense mutations. *Nature Methods* **7**:248.
- Andersson ML, Eliasson E and Lindh JD (2012) A clinically significant interaction between warfarin and simvastatin is unique to carriers of the CYP2C9*3 allele. *Pharmacogenomics* **13**:757-762.
- Backes WL and Kelley RW (2003) Organization of multiple cytochrome P450s with NADPH-cytochrome P450 reductase in membranes. *Pharmacol Ther* **98**:221-233.
- Bielinski SJ, Olson JE, Pathak J, Weinshilboum RM, Wang L, Lyke KJ, Ryu E, Targonski PV, Van Norstrand MD, Hathcock MA, Takahashi PY, McCormick JB, Johnson KJ, Maschke KJ, Rohrer Vitek CR, Ellingson MS, Wieben ED, Farrugia G, Morrisette JA, Kruckeberg KJ, Bruflat JK, Peterson LM, Blommel JH, Skierka JM, Ferber MJ, Black JL, Baudhuin LM, Klee EW, Ross JL, Veldhuizen TL, Schultz CG, Caraballo PJ, Freimuth RR, Chute CG and Kullo IJ (2014) Preemptive genotyping for personalized medicine: design of the right drug, right dose, right time-using genomic data to individualize treatment protocol. *Mayo Clin Proc* **89**:25-33.
- Cheng Q, Sohl CD and Guengerich FP (2009) High-throughput fluorescence assay of cytochrome P450 3A4. *Nat Protoc* **4**:1258-1261.
- Choi Y and Chan AP (2015) PROVEAN web server: a tool to predict the functional effect of amino acid substitutions and indels. *Bioinformatics* **31**:2745-2747.
- D. RP, P. WJ, G. AP and S. PR (2008) Sub one minute inhibition assays for the major cytochrome P450 enzymes utilizing ultra-performance liquid chromatography/tandem mass spectrometry. *Rapid Commun Mass Spectrom* **22**:1345-1350.
- Dai DP, Wang SH, Geng PW, Hu GX and Cai JP (2014a) In vitro assessment of 36 CYP2C9 allelic isoforms found in the Chinese population on the metabolism of glimepiride. *Basic Clin Pharmacol Toxicol* **114**:305-310.
- Dai DP, Wang SH, Li CB, Geng PW, Cai J, Wang H, Hu GX and Cai JP (2015) Identification and Functional Assessment of a New CYP2C9 Allelic Variant CYP2C9*59. *Drug Metab Dispos* **43**:1246-1249.
- Dai DP, Xu RA, Hu LM, Wang SH, Geng PW, Yang JF, Yang LP, Qian JC, Wang ZS, Zhu GH, Zhang XH, Ge RS, Hu GX and Cai JP (2014b) CYP2C9 polymorphism analysis in Han Chinese populations: building the largest allele frequency database. *Pharmacogenomics J* **14**:85-92.
- DeLozier TC, Lee S-C, Coulter SJ, Goh BC and Goldstein JA (2005) Functional characterization of novel allelic variants of CYP2C9 recently discovered in southeast Asians. *J Pharmacol Exp Ther* **315**:1085-1090.
- Deng M, Yang X, Qin B, Liu T, Zhang H, Guo W, Lee SB, Kim JJ, Yuan J, Pei H, Wang L and Lou Z (2016) Deubiquitination and Activation of AMPK by USP10. *Mol Cell* **61**:614-624.
- Dresser GK, Spence JD and Bailey DG (2000) Pharmacokinetic-pharmacodynamic consequences and clinical relevance of cytochrome P450 3A4 inhibition. *Clin Pharmacokinet* **38**:41-57.
- Flanagan SE, Patch A-M and Ellard S (2010) Using SIFT and PolyPhen to Predict Loss-of-Function and Gain-of-Function Mutations. *Genet Test Mol Biomarkers* **14**:533-537.
- Friedman MA, Woodcock J, Lumpkin MM, Shuren JE, Hass AE and Thompson LJ (1999) The safety of newly approved medicines: Do recent market removals mean there is a problem? *JAMA* **281**:1728-1734.
- G. AP, S. PR, D. JM, D. RP and Darcy S (2010) A rapid ultra-performance liquid chromatography/tandem mass spectrometric methodology for the in vitro analysis of Pooled and Cocktail cytochrome P450 assays. *Rapid Commun Mass Spectrom* **24**:147-154.

DMD # 84269

- Gonzalez FJ and Korzekwa KR (1995) Cytochromes P450 expression systems. *Annu Rev Pharmacol Toxicol* **35**:369-390.
- Gotoh O (1992) Substrate recognition sites in cytochrome P450 family 2 (CYP2) proteins inferred from comparative analyses of amino acid and coding nucleotide sequences. *J Biol Chem* **267**:83-90.
- Guo X, Chavez A, Tung A, Chan Y, Kaas C, Yin Y, Cecchi R, Garnier SL, Kelsic ED, Schubert M, DiCarlo JE, Collins JJ and Church GM (2018) High-throughput creation and functional profiling of DNA sequence variant libraries using CRISPR-Cas9 in yeast. *Nat Biotechnol*.
- Haller G, Alvarado D, McCall K, Mitra RD, Dobbs MB and Gurnett CA (2016) Massively parallel single-nucleotide mutagenesis using reversibly terminated inosine. *Nature Methods* **13**:923.
- Hu GX, Pan PP, Wang ZS, Yang LP, Dai DP, Wang SH, Zhu GH, Qiu XJ, Xu T, Luo J, Lian QQ, Ge RS and Cai JP (2015) In Vitro and In Vivo Characterization of 13 CYP2C9 Allelic Variants Found in Chinese Han Population. *Drug Metabolism and Disposition* **43**:561-569.
- Ingelman-Sundberg M and Rodriguez-Antona C (2005) Pharmacogenetics of drug-metabolizing enzymes: implications for a safer and more effective drug therapy. *Philos Trans R Soc Lond B Biol Sci* **360**:1563-1570.
- Ingelman-Sundberg M, Sim SC, Gomez A and Rodriguez-Antona C (2007) Influence of cytochrome P450 polymorphisms on drug therapies: pharmacogenetic, pharmacoeconomic and clinical aspects. *Pharmacol Ther* **116**:496-526.
- Ji Y, Moon I, Zlatkovic J, Salavaggione OE, Thomae BA, Eckloff BW, Wieben ED, Schaid DJ and Weinshilboum RM (2007) Human Hydroxysteroid Sulfotransferase SUL2B1 Pharmacogenomics: Gene Sequence Variation and Functional Genomics. *J Pharmacol Exp Ther* **322**:529-540.
- Ji Y, Skierka JM, Blommel JH, Moore BE, VanCuyk DL, Bruflat JK, Peterson LM, Veldhuizen TL, Fadra N, Peterson SE, Lagerstedt SA, Train LJ, Baudhuin LM, Klee EW, Ferber MJ, Bielinski SJ, Caraballo PJ, Weinshilboum RM and Black JL, 3rd (2016) Preemptive Pharmacogenomic Testing for Precision Medicine: A Comprehensive Analysis of Five Actionable Pharmacogenomic Genes Using Next-Generation DNA Sequencing and a Customized CYP2D6 Genotyping Cascade. *J Mol Diagn* **18**:438-445.
- Kariv I, Fereshteh MP and Oldenburg KR (2001) Development of a Miniaturized 384-Well High Throughput Screen for the Detection of Substrates of Cytochrome P450 2D6 and 3A4 Metabolism. *J Biomol Screen* **6**:91-99.
- Kim K, Park P, Hong S and Park JY (2008) The effect of CYP2C19 polymorphism on the pharmacokinetics and pharmacodynamics of clopidogrel: a possible mechanism for clopidogrel resistance. *Clin Pharmacol Ther* **84**:236-242.
- Kirchheiner J, Nickchen K, Bauer M, Wong M, Licinio J, Roots I and Brockmüller J (2004) Pharmacogenetics of antidepressants and antipsychotics: the contribution of allelic variations to the phenotype of drug response. *Mol Psychiatry* **9**:442.
- Lee HI, Bae JW, Choi CI, Lee YJ, Byeon JY, Jang CG and Lee SY (2014) Strongly increased exposure of meloxicam in CYP2C9*3/*3 individuals. *Pharmacogenet Genomics* **24**:113-117.
- Li F, Wang L, Burgess RJ and Weinshilboum RM (2008) Thiopurine S-methyltransferase pharmacogenetics: autophagy as a mechanism for variant allozyme degradation. *Pharmacogenet Genomics* **18**:1083-1094.
- Liu D, Ho MF, Schaid DJ, Scherer SE, Kalari K, Liu M, Biernacka J, Yee V, Evans J, Carlson E, Goetz MP, Kubo M, Wickerham DL, Wang L, Ingle JN and Weinshilboum RM (2017) Breast cancer chemoprevention pharmacogenomics: Deep sequencing and functional genomics of the ZNF423 and CTSO genes. *NPJ breast cancer* **3**:30.
- Mark C, Jim D, Martin D, Leila E, Tom F, Sue H, Tim H, Luke J, Nick M, Jeanna M-P, Gil M, Katrina N-R, Matthew P, Vivienne P, Augusto R, Laura R, Clare T and Kerrie W (2017) *The 100,000 Genomes Project Protocol*.

DMD # 84269

- Min L, Nie M, Zhang A, Wen J, Noel SD, Lee V, Carroll RS and Kaiser UB (2016) Computational analysis of missense variants of G protein-coupled receptors involved in the neuroendocrine regulation of reproduction. *Neuroendocrinology* **103**:230-239.
- Murphy MP (2000) Current pharmacogenomic approaches to clinical drug development. *Pharmacogenomics* **1**:115-123.
- Naccarella F and Bracchetti D (1986) [Arrhythmogenic right ventricle: isolated right dysplasia or diffused myocardial pathology? A diagnostic protocol for evaluating its prevalence and differentiating it from other conditions of an arrhythmogenic ventricle]. *G Ital Cardiol* **16**:750-754.
- Negishi M, Iwasaki M, Juvonen RO, Sueyoshi T, Darden TA and Pedersen LG (1996) Structural flexibility and functional versatility of cytochrome P450 and rapid evolution. *Mutation Research/Fundamental and Molecular Mechanisms of Mutagenesis* **350**:43-50.
- Niinuma Y, Saito T, Takahashi M, Tsukada C, Ito M, Hirasawa N and Hiratsuka M (2014) Functional characterization of 32 CYP2C9 allelic variants. *The pharmacogenomics journal* **14**:107.
- Peng Y, Wu H, Zhang X, Zhang F, Qi H, Zhong Y, Wang Y, Sang H, Wang G and Sun J (2015) A comprehensive assay for nine major cytochrome P450 enzymes activities with 16 probe reactions on human liver microsomes by a single LC/MS/MS run to support reliable in vitro inhibitory drug-drug interaction evaluation. *Xenobiotica* **45**:961-977.
- Pereira NL, Aksoy P, Moon I, Peng Y, Redfield MM, Burnett JC, Jr., Wieben ED, Yee VC and Weinshilboum RM (2010) Natriuretic peptide pharmacogenetics: membrane metallo-endopeptidase (MME): common gene sequence variation, functional characterization and degradation. *J Mol Cell Cardiol* **49**:864-874.
- Prieto-Perez R, Ochoa D, Cabaleiro T, Roman M, Sanchez-Rojas SD, Talegon M and Abad-Santos F (2013) Evaluation of the relationship between polymorphisms in CYP2C8 and CYP2C9 and the pharmacokinetics of celecoxib. *J Clin Pharmacol* **53**:1261-1267.
- Scott SA, Sangkuhl K, Gardner EE, Stein CM, Hulot JS, Johnson JA, Roden DM, Klein TE and Shuldiner AR (2011) Clinical Pharmacogenetics Implementation Consortium guidelines for cytochrome P450-2C19 (CYP2C19) genotype and clopidogrel therapy. *Clin Pharmacol Ther* **90**:328-332.
- Scott SA, Sangkuhl K, Stein CM, Hulot JS, Mega JL, Roden DM, Klein TE, Sabatine MS, Johnson JA and Shuldiner AR (2013) Clinical Pharmacogenetics Implementation Consortium guidelines for CYP2C19 genotype and clopidogrel therapy: 2013 update. *Clin Pharmacol Ther* **94**:317-323.
- Sim N-L, Kumar P, Hu J, Henikoff S, Schneider G and Ng PC (2012) SIFT web server: predicting effects of amino acid substitutions on proteins. *Nucleic Acids Res* **40**:W452-W457.
- Sim S, Kacevska M and Ingelman-Sundberg M (2013) Pharmacogenomics of drug-metabolizing enzymes: a recent update on clinical implications and endogenous effects. *The pharmacogenomics journal* **13**:1.
- Straub P, Lloyd M, Johnson EF and Kemper B (1994) Differential effects of mutations in substrate recognition site 1 of cytochrome P450 2C2 on lauric acid and progesterone hydroxylation. *Biochemistry* **33**:8029-8034.
- Stresser DM, Blanchard AP, Turner SD, Erve JCL, Dandeneau AA, Miller VP and Crespi CL (2000) Substrate-Dependent Modulation of CYP3A4 Catalytic Activity: Analysis of 27 Test Compounds with Four Fluorometric Substrates. *Drug Metabolism and Disposition* **28**:1440-1448.
- V Trubetskoy O, R Gibson J and D Marks B (2005) *Highly Miniaturized Formats for In Vitro Drug Metabolism Assays Using Vivid(R) Fluorescent Substrates and Recombinant Human Cytochrome P450 Enzymes*.
- Wang L, Nguyen TV, McLaughlin RW, Sikkink LA, Ramirez-Alvarado M and Weinshilboum RM (2005) Human thiopurine S-methyltransferase pharmacogenetics: variant allozyme misfolding and aggresome formation. *Proc Natl Acad Sci U S A* **102**:9394-9399.

DMD # 84269

- Wang L, Sullivan W, Toft D and Weinshilboum R (2003) Thiopurine S-methyltransferase pharmacogenetics: chaperone protein association and allozyme degradation. *Pharmacogenetics* **13**:555-564.
- Wang L, Yee VC and Weinshilboum RM (2004) Aggresome formation and pharmacogenetics: sulfotransferase 1A3 as a model system. *Biochem Biophys Res Commun* **325**:426-433.
- Weinshilboum R (2003) Inheritance and drug response. *N Engl J Med* **348**:529-537.
- Weinshilboum RM, Otterness DM and Szumlanski CL (1999) Methylation pharmacogenetics: catechol O-methyltransferase, thiopurine methyltransferase, and histamine N-methyltransferase. *Annu Rev Pharmacol Toxicol* **39**:19-52.
- Weinshilboum RM and Wang L (2017) Pharmacogenomics: Precision Medicine and Drug Response. *Mayo Clin Proc* **92**:1711-1722.
- Wester MR, Yano JK, Schoch GA, Yang C, Griffin KJ, Stout CD and Johnson EF (2004) The structure of human cytochrome P450 2C9 complexed with flurbiprofen at 2.0-Å resolution. *J Biol Chem* **279**:35630-35637.
- Yamazaki H, Nakamura M, Komatsu T, Ohyama K, Hatanaka N, Asahi S, Shimada N, Guengerich FP, Shimada T, Nakajima M and Yokoi T (2002) Roles of NADPH-P450 Reductase and Apo- and Holo-Cytochrome b5 on Xenobiotic Oxidations Catalyzed by 12 Recombinant Human Cytochrome P450s Expressed in Membranes of Escherichia coli. *Protein Expr Purif* **24**:329-337.

Footnotes: (Support)

This work was supported in part by Mayo Cancer Center Support Grant CA 15083; NIH grants [U19 GM61388, RO1 GM28157, RO1 GM125633, and U01 HG06379]; The Pharmacogenomics Program of the Mayo Clinic Center for Individualized Medicine; The Mayo Clinic Robert D. and Patricia E. Kern Center for the Science of Healthcare Delivery and the Mayo Clinic Center for Individualized Medicine. Dr. John L. Black has licensed intellectual property to the companies AssureX Health and OneOme. In addition, he has stock ownership in OneOme. Drs. Weinshilboum and Wang are co-founders and stockholders in OneOme.

DMD # 84269

Legends for Figures

Figure 1, (A) Quantitative Western blot analysis of newly identified variants in CYP2C9 and CYP2C19 (* $p \leq 0.05$, *** $p < 0.001$ vs WT). **(B)** Effect of MG132 treatment on the protein levels of CYP2C9 and CYP2C19. All values are mean \pm S.E.M for three separate independent assays. ANOVA was performed to compare gene expression, followed by multiple comparison tests for individual comparisons when significant effects were detected. * $p \leq 0.05$, *** $p \leq 0.001$.

Figure 2, (A) Relative CYP2C9 Vivid[®] Enzyme Activity: Bar graphs showing normalized Vivid[®] enzymatic activity of the CYP2C9 wild-type and variant proteins (nM fluorescent product formed/ min/ mg total protein) (error bars depict standard deviation of the mean in three independent activity assays). **(B)** Relative CYP2C19 Vivid[®] Enzyme Activity: Bar graphs showing normalized Vivid[®] enzymatic activity of the CYP2C19 wild-type and variant proteins (nM fluorescent product formed/ min/ mg total protein) (error bars depict standard deviation of the mean in three experimental samples). Enzyme activity was analyzed using one-way ANOVA, with mean comparison for each variant genotype against the wildtype control performed using Dunnet's test. Corresponding p-values were multiplicity-adjusted and reported as such. * $p \leq 0.05$, ** $p \leq 0.01$, *** $p \leq 0.001$.

Figure 3, (A) CYP2C9 Vivid[®] Enzyme Activity vs Protein Content: Correlation of recombinant protein quantity vs Vivid[®] enzyme activity for CYP2C9 variant allozymes. The Normalized

DMD # 84269

protein quantities are plotted on the horizontal axis and the Normalized Vivid[®] enzyme activities are plotted on the vertical axis. $R^2=0.693$ and P value=0.0015. **(B)** CYP2C19 Vivid[®] Enzyme Activity vs Protein Content: Correlation of recombinant protein quantity vs Vivid[®] enzyme activity for CYP2C19 variant allozymes. The Normalized protein quantities are plotted on the horizontal axis and the Normalized Vivid[®] enzyme activities are plotted on the vertical axis. $R^2=0.825$ and P value=0.0003. Associations between protein content and enzyme activity were evaluated using Pearson correlations, with two-sided t-test p-values reported. The solid line illustrates the line of identity for the association between normalized activity and protein content.

Figure 4, **(A)** Michaelis Menten curves of the enzymatic activities of the recombinant wild-type and 10 variant CYP2C9 allozymes (including CYP2C9*3) toward tolbutamide (each point represents the mean \pm SD of three separate experiments). **(B)** Michaelis Menten curves of the enzymatic activities of the recombinant wild-type and 8 variant CYP2C19 protein (including CYP2C19*3) toward (S)-mephenytoin (each point represents the mean \pm SD of three separate experiments). Enzyme kinetics were modeled using non-linear regression based on the Michaelis-Menten equation.

Figure 5, **(A)** Correlation analysis between enzyme activities determined by high throughput assay vs velocity of product formation determined by mass spectrometric assay for CYP2C9 variant allozymes. Relative velocity of hydroxy tolbutamide formation (nmole product formed/ mL/ min) at 50 μ M tolbutamide concentration are plotted on the horizontal axis and the Relative enzyme activity values determined by Vivid[®] assay (nM fluorescent product formed/ min/ mg

DMD # 84269

total protein) are plotted on the vertical axis. $R^2 = 0.907$ and P value = <0.0001 . **(B)** Correlation analysis between enzyme activities determined by high throughput assay vs velocity of product formation determined by mass spectrometric assay for CYP2C19 Variants. Relative velocity of (S)-4-hydroxy mephenytoin formation (nmole product formed/ mL/ min) at $1000\mu\text{M}$ at (S)-mephenytoin concentration are plotted on the horizontal axis and the Relative Vivid[®] enzyme activity values determined by Vivid[®] assay (nM fluorescent product formed/ min/ mg total protein) are plotted on the vertical axis. $R^2 = 0.898$ and P value = <0.0001 . Associations between protein content and enzyme activity were evaluated using Pearson correlations, with two-sided t -test p -values reported. The solid line illustrates the line of identity for the association between enzyme activities determined by high throughput assay and intrinsic clearance determined by mass spectrometric assay.

DMD # 84269

Table 1: CYP2C9 and CYP2C19 variants cDNA and Encoded AA Changes

Gene	cDNA changes	Amino acid changes (Protein)	Comments
CYP2C9	218C>T	Pro73Leu	Found with heterozygous CYP2C9 *2
CYP2C9	229C>A	Leu77Met	
CYP2C9	343A>C	Ser115Arg	
CYP2C9	707delA	Asn236Thrfs*5	
CYP2C9	709G>C	Val237Leu	
CYP2C9	791T>C	Ile264Thr	
CYP2C9	801C>T	Phe267Phe	
CYP2C19	65A>G	Gln22Arg	Found with heterozygous CYP2C19 *17
CYP2C19	337G>A	Val113Ile	Found with heterozygous CYP2C19 *2 and *17
CYP2C19	518C>T	Ala173Val	Found with heterozygous CYP2C19 *2
CYP2C19	556C>T	Arg186Cys	Found with homozygous CYP2C19 *2
CYP2C19	557G>A	Arg186His	Found with homozygous CYP2C19 *2
CYP2C19	578A>G	Gln193Arg	Found with heterozygous CYP2C19 *2
CYP2C19	815A>G	Glu272Gly	

DMD # 84269

Table 2: Data search results for *CYP2C9* and *CYP2C19* variants in gnomAD data bank.

Gene	cDNA changes	dbSNP data bank		gnomAD
		rsIDs	Validation	Minor allele frequency (MAF)
CYP2C9	218C>T	rs762081829	Not done	5.69E-05
CYP2C9	229C>A	Not present		Not recorded
CYP2C9	343A>C	rs771237265	1	1.01E-04
CYP2C9	707delA	rs549167718	2	4.099E-06*
CYP2C9	709G>C	Not present		Not recorded**
CYP2C9	791T>C	rs761895497	1	1.09E-05
CYP2C9	801C>T	rs149158426	1,2,3	8.55E-04
CYP2C19	65A>G	rs144928727	3	1.22E-05
CYP2C19	337G>A	rs145119820	1,2,3	2.24E-04
CYP2C19	518C>T	rs61311738	1,2,3	4.66E-03
CYP2C19	556C>T	rs183701923	1,2,3	9.74E-05
CYP2C19	557G>A	rs140278421	1,2,3	1.08E-04
CYP2C19	578A>G	Not present		4.06E-06
CYP2C19	815A>G	Not present		Not recorded

Data base search results are obtained from <http://gnomad.broadinstitute.org/> and <https://www.ncbi.nlm.nih.gov/projects/SNP/> as of August 2018.

1- Validated by frequency or genotype data: minor alleles observed in at least two chromosomes

2- SNP has been sequenced in 1000 genome project

3- Validated by multiple, independent submissions to the refSNP cluster

*(without frameshift)

** (other mutations to Ile, Phe, Val and Ala recorded at this position)

DMD # 84269

Table 3: Enzyme Kinetic properties of recombinant wild-type and mutant CYP2C9 proteins for tolbutamide hydroxylation and *In silico* Functional Prediction of CYP2C9 Variants.

cDNA	V _{max} ± SD X 10 ⁻³ (nmole/mg/min)	K _m ± SD (μM)	CL _{INT} X 10 ⁻⁴ (μl/mgprotein/min) (relative CL _{INT} (%wild-type))	Polyphen	SIFT	PROVEAN	Enzyme activity in relation to WT		Concordance Y/N
							Vivid (%)*	MS (%)*	
WT	13.5 ± 0.64	51 ± 10.51	2.71 ± 0.41						
218C>T	4.11 ± 0.22	67.8 ± 16.1	0.62 ± 0.11 (23%)**	probably damaging	Damaging	Deleterious	31	23	YES
229C>A	17.7 ± 0.61	76.2 ± 7.49	2.33 ± 0.16(86%)	probably damaging	Damaging	Neutral	88	86	NO
343A>C	7.12 ± 0.79	283 ± 49.2	0.26 ± 0.04(9.6%)**	probably damaging	Damaging	Deleterious	11	10	YES
707_delA	0.42 ± 0.04	141 ± 183		possibly damaging	N/A	N/A	0	0	N/A
709G>C	13.9 ± 3.36	219 ± 127	0.73 ± 0.24(29%)**	benign	Tolerated	Neutral	26	27	NO
707_709delinsCC	0.06				N/A	N/A			N/A
791T>C	5.83 ± 0.41	50.1 ± 5.62	1.17 ± 0.09(43.6%)*	possibly damaging	Tolerated	Deleterious	72	43	YES
801C>T	14.7 ± 0.46	56.5 ± 10.6	2.66 ± 0.42(98.1%)		Tolerated	Neutral	111	98	YES
*3	2.80 ± 0.81	149 ± 157	0.32 ± 0.24(10.3%)**				1	10	

The kinetic parameters for tolbutamide hydroxylation of CYP2C9 variants 707delA and 707_709delinsCC (Naccarella and Bracchetti) could not be determined because the amount of produced metabolite was at or below the detection limit at the lower substrate concentrations.

The kinetic parameters for tolbutamide hydroxylation of 4 variants. These data represent the mean ± SD of three independently performed catalytic assays. Concordance, defined as agreement of the kinetic assay result with at least two of three *in silico* software results. V_{max}, velocity maximum; CL_{INT}, intrinsic clearance; K_m, Michaelis constant; SD, standard deviation; N/A- Not applicable. *P<0.05, **P<0.01 compared to CYP2C9 WT.

DMD # 84269

Table 4: Enzyme Kinetic properties of recombinant wild-type and mutant CYP2C19 proteins for (S)-mephenytoin hydroxylation and *In silico* Functional Prediction of CYP2C19 Variants

cDNA	Vmax ± SD X 10 ⁻³ (nmole/mg/min)	Km ± SD (μM)	CL _{INT} X 10 ⁻⁴ (μl/mgprotein/min) (% of wild-type)	Polyphen	SIFT	PROVEAN	Enzyme activity in relation to WT		Concor dance
							Vivid (%)*	MS (%)*	Y/N
WT	67.2 ± 2.51	30.1 ± 7.79	23.4 ± 6.27						
65A>G	33.3 ± 0.74	40.3 ± 0.86	8.25 ± 0.36(36.2%)	Benign	Tolerated	Deleterious	49	36	NO
337G>A	23.6 ± 2.75	96.6 ± 23.1	2.49 ± 0.28(10.7%)*	Benign	Tolerated	Neutral	75	11	NO
518C>T	3.65 ± 0.25	205 ± 11.8	0.18 ± 0.02(0.7%)*	Probably Damaging	Tolerated	Deleterious	5	1	YES
556C>T	3.03 ± 0.36	148 ± 69.5	0.23 ± 0.09(1.6%)*	Probably Damaging	Damaging	Deleterious	7	2	YES
557G>A	4.33 ± 0.34	30.5 ± 7.12	1.45 ± 0.20(6.5%)*	Probably Damaging	Tolerated	Deleterious	7	7	YES
578A>G	68.5 ± 4.69	51.5 ± 7.69	13.4 ± 1.06(57.9 %)	Benign	Tolerated	Neutral	106	58	YES
815A>G	35.2 ± 0.11	38.4 ± 2.47	9.19 ± 0.54(39.7%)	Benign	Damaging	Deleterious	53	40	YES
3	0.02 ± 0.01	4.82 ± 0.00	0.05 ± 0.02(0.2%)				3	N/A	

The kinetic parameters for (S)-mephenytoin hydroxylation of variants 518C>CT, 556C>CT and *3 could not be determined because the amount of produced metabolite was at or below the detection limit at the lower substrate concentrations. These data represent the mean ± SD of three independently performed catalytic assays. Concordance, defined as agreement of the kinetic assay result with at least two of three *in silico* software results. Vmax, velocity maximum; CL_{INT}, intrinsic clearance; Km, Michaelis constant; SD, standard deviation; N/A- Not applicable.

*P<0.05 compared to CYP2C19 WT.

Figure 1

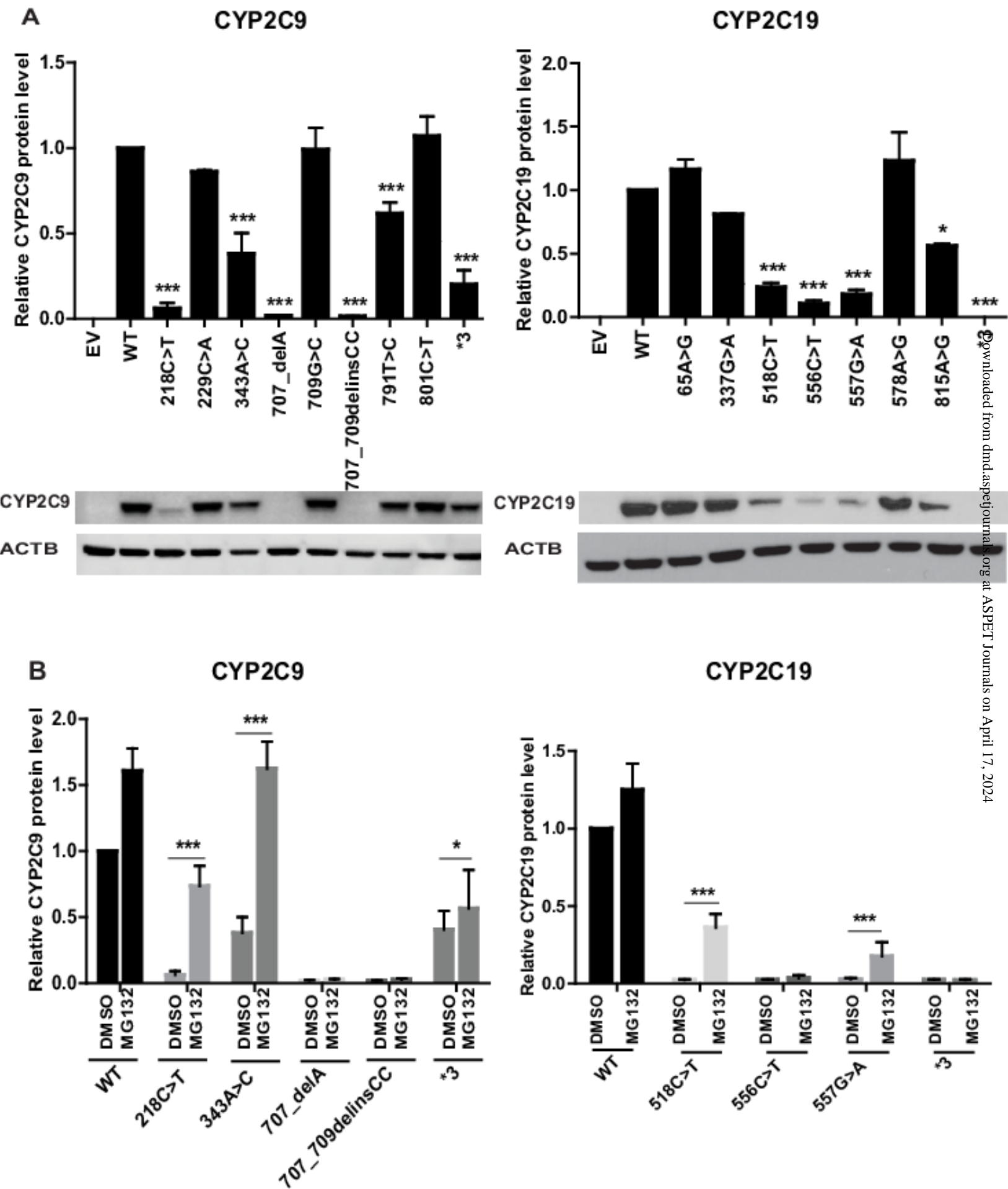


Figure 2

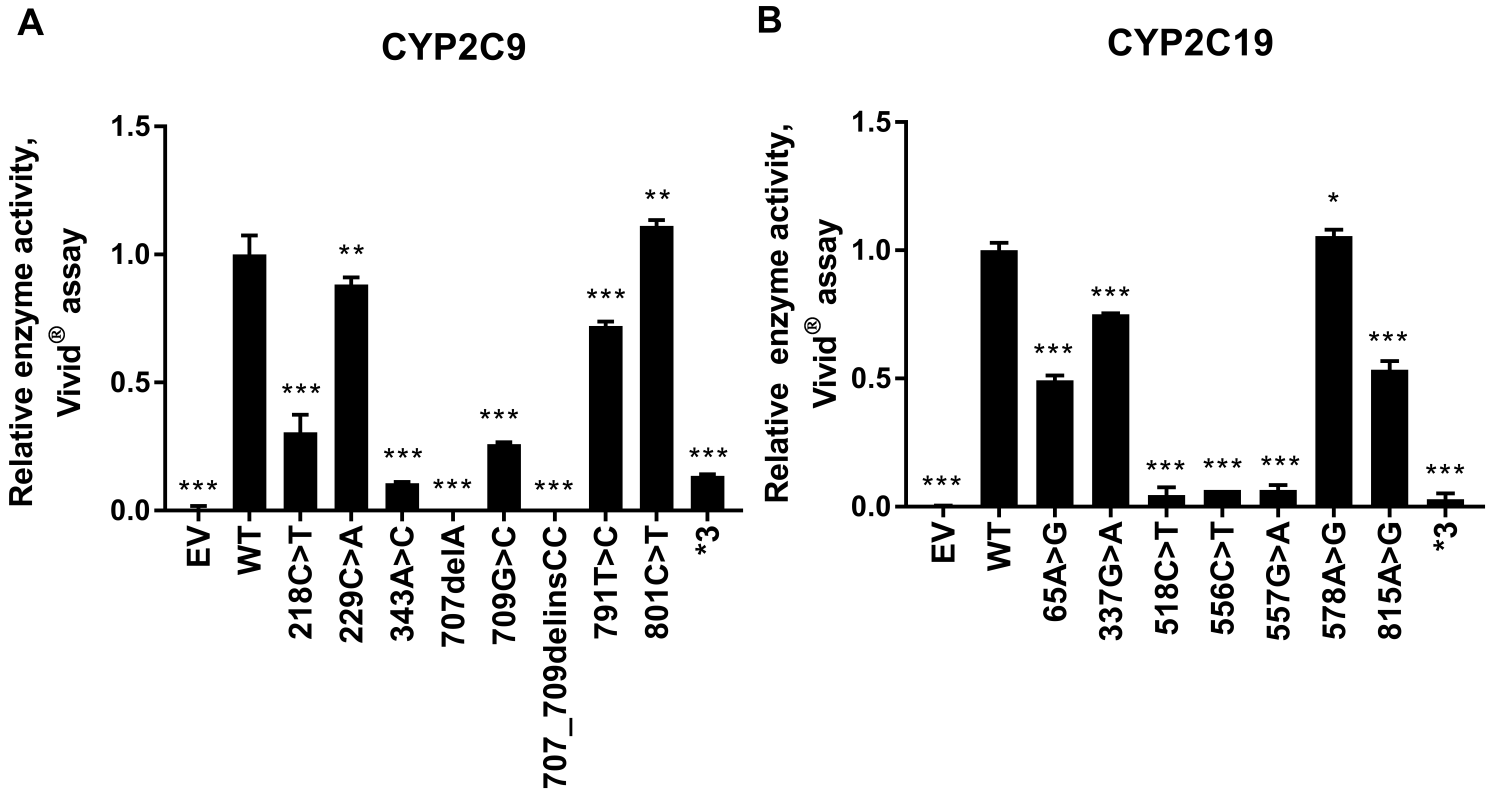


Figure 3

DMD Fast Forward. Published on February 11, 2019 as DOI: 10.1124/dmd.118.084269
This article has not been copyedited and formatted. The final version may differ from this version.

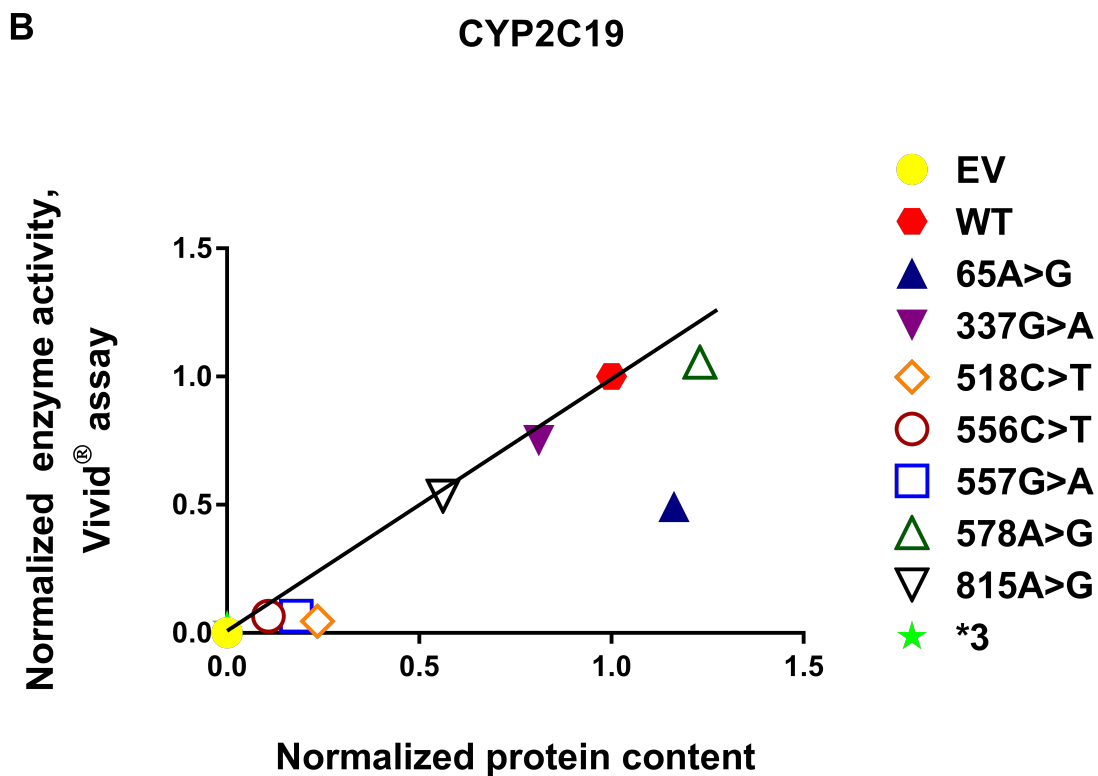
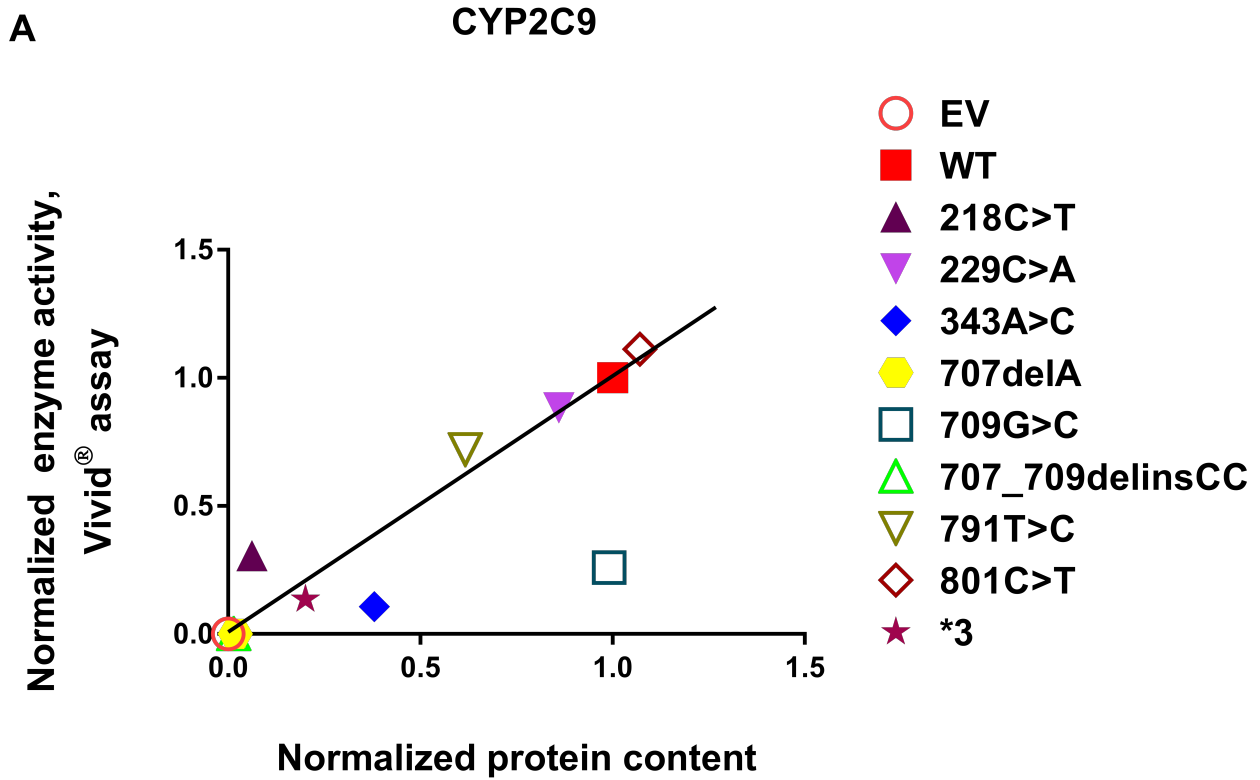


Figure 4

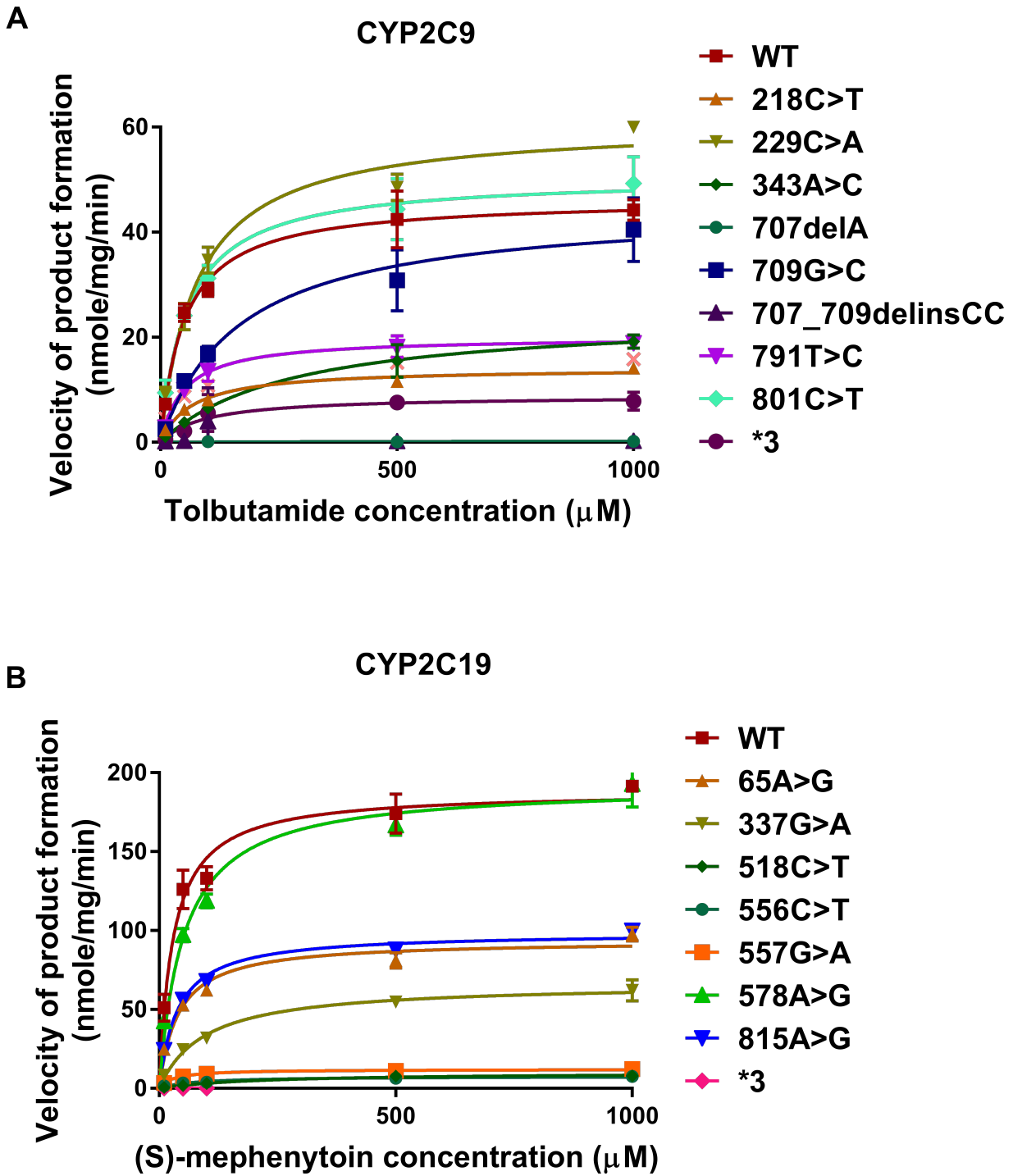


Figure 5

DMD Fast Forward. Published on February 11, 2019 as DOI: 10.1124/dmd.118.084269
This article has not been copyedited and formatted. The final version may differ from this version.

